JOURNAL OF AGRICULTURAL AND FOOD CHEMISTRY

Multiple Forms of Xylose Reductase in *Candida intermedia*: Comparison of Their Functional Properties Using Quantitative Structure−Activity Relationships, Steady-State Kinetic Analysis, and pH Studies

BERND NIDETZKY,*,‡ KASPAR BRÜGGLER,# REGINA KRATZER,‡ AND PETER MAYR#

Institute of Biotechnology, Graz University of Technology, Petersgasse 12/I, A-8010 Graz, Austria, and Institute of Food Technology, University of Agricultural Sciences, Muthgasse 18, A-1190 Vienna, Austria

The xylose-fermenting yeast *Candida intermedia* produces two isoforms of xylose reductase: one is NADPH-dependent (monospecific xylose reductase; msXR), and another is shown here to prefer NADH ≈4-fold over NADPH (dual specific xylose reductase; dsXR). To compare the functional properties of the isozymes, a steady-state kinetic analysis for the reaction D-xylose + NAD(P)H + H^+ ↔ xylitol + $NAD(P)^+$ was carried out and specificity constants ($k_{cat}/K_{aldehyde}$) were measured for the reduction of a series of aldehydes differing in side-chain size as well as hydrogen-bonding capabilities with the substrate binding pocket of the enzyme. dsXR binds $NAD(P)^+$ ($K_{iNAD+} = 70\ \mu M$; $K_{iNADP+} = 55\ \mu M$) weakly and NADH ($K_i = 8\ \mu M$) about as tightly as NADPH ($K_i = 14\ \mu M$). msXR shows uniform binding of NADPH and $NADP^+$ ($K_{iNADP+} \approx K_{iNADPH} = 20\ \mu M$). A quantitative structure−activity relationship analysis was carried out by correlating logarithmic $k_{cat}/K_{aldehyde}$ values for dsXR with corresponding logarithmic $k_{cat}/K_{aldehyde}$ values for msXR. This correlation is linear with a slope of ≈1 ($r^2 = 0.912$), indicating that no isozyme-related pattern of substrate specificity prevails and aldehyde-binding modes are identical in both XR forms. Binary complexes of dsXR−NADH and msXR−NADPH show the same macroscopic pK of ≈9.0−9.5, above which the activity is lost in both enzymes. A lower pK of 7.4 is seen for dsXR−NADPH. Specificity for NADH and greater binding affinity for $NAD(P)H$ than $NAD(P)^+$ are thus the main features of enzymic function that distinguish dsXR from msXR.

KEYWORDS: Isozymes; dual coenzyme specificity; binding affinity; xylose utilization; xylose fermentation

INTRODUCTION

D-xylose is the main constituent monosaccharide of plant hemicellulose. The vast amounts of hemicellulose-containing raw materials accumulating as process wastes in agriculture and forestry make D-xylose a potential source for production of large-volume commodities such as fuel ethanol (*1*). Yeast fermentation of D-xylose has therefore attracted considerable interest in biotechnological research (*1*−*3*). The initial catabolic pathway for xylose in yeast is contributed by two oxidoreductases, xylose reductase [XR; alditol:$NAD(P)^+$ 1-oxidoreductase; EC 1.1.1.21] and xylitol dehydrogenase (XDH; alditol:NAD^+ 2-oxidoreductase; EC 1.1.1.9) (*1*−*3*). XR catalyzes the first step by reducing the C1 carbonyl group of xylose, yielding xylitol as the product (*4*). Xylitol is then oxidized by XDH to give D-xylulose (*5*). Because XDH requires NAD^+ whereas XR generally prefers NADPH over NADH, the pathway is not balanced in respect to the redox cofactors involved. Consequently, formation of fermentation byproducts such as glycerol and xylitol occurs and reflects the need for balancing the pools of NAD^+/NADH and $NADP^+$/NADPH, respectively. Obviously, this will lower ethanol yield from xylose (reviewed in ref *1*). Therefore, NADH-linked activity of XR is an important physiological and technological requirement for efficient yeast xylose fermentation (*1* and references cited therein). If XR used NADH rather than NADPH, cofactor imbalances during xylose conversion under oxygen-limited conditions might be alleviated substantially.

Biochemical work from different laboratories has shown that yeast XRs can be classified according to coenzyme specificity into a group of NADPH-specific reductases (monospecific XR; msXR) and another enzyme group active with NADPH and NADH (dual specific XR; dsXR) (*4*; reviewed in refs *6* and *7*). dsXR is present in all yeast taxae known to ferment xylose such as *Pichia stipitis*, *Candida shehatae*, *Candida tenuis*, and *Pachysolen tannophilus* (*1* and references cited therein). Both msXR and dsXR are homodimers composed of identical subunits of ≈36 kDa molecular mass (*4*, *6*, *7*). The available

* Corresponding author (telephone +43-316-873-8400; fax +43-316-873-8434; e-mail bernd.nidetzky@tugraz.at).
‡ Graz University of Technology.
# University of Agricultural Sciences.

10.1021/jf034426j CCC: $25.00
Published on Web 12/02/2003

sequence information for XR enzymes that have been characterized at the protein level (*6*, *7*) indicates that primary structures of msXR and dsXR share a quite high entire-chain similarity (≈70%). To understand their relative roles in xylose fermentation, the functional properties of dsXR and msXR must be known in detail.

We report here a detailed comparison of msXR and dsXR from the xylose-fermenting yeast *Candida intermedia*. This yeast system was chosen because, first of all, *C. intermedia* is a good natural producer of ethanol from xylose (*8*). *C. intermedia* msXR and dsXR activities are induced in the presence of D-xylose and repressed in the presence of D-glucose (P.M. and B.N., unpublished results), emphasizing a common major function of the isozymes in the metabolism of xylose. Second, there is the considerable advantage that msXR and dsXR occur at the same time in a single organism. A rigorous comparative evaluation of XR isoforms is thus possible in the absence of complexity due to different microbial species, one producing msXR and another producing dsXR (*4*). Third, a preliminary characterization of *C. intermedia* dsXR has revealed that unlike other dsXRs purified and characterized biochemically so far, this enzyme prefers NADH over NADPH (*9*). Although there is good evidence that NADPH-preferring dsXR can effectively utilize NADH, it is not completely clear to what extent this occurs in vivo. This reinforces the potential utility of a NADH-preferring dsXR.

Our comparison is based on (i) a full steady-state kinetic analysis for each isozyme in regard to the natural, NADPH- or NADH-dependent reaction with D-xylose, (ii) a detailed characterization of the substrate specificities of the two XR isoforms coupled to a quantitative structure−activity relationship analysis through which we measure the similarity between the aldehyde binding pockets of msXR and dsXR, and (iii) pH effects on the enzymic reduction of xylose. Therefore, functional properties of msXR and dsXR are examined in respect to enzyme interactions with both the substrate and the coenzyme, and a comprehensive picture results.

MATERIALS AND METHODS

Materials. msXR and dsXR from *C. intermedia* (also named *Kluyveromyces cellobiovorus*) were produced and purified to apparent homogeneity as described recently (*9*). All used substrates were of the highest purity available and obtained from Sigma-Aldrich or Fluka.

Kinetic Measurements. Apparent kinetic parameters, that is, the turnover number k_{cat} (s^{-1}) and the apparent Michaelis constant $K_{aldehyde}$ (mM), for the NAD(P)H-dependent reduction of different aldehydes by msXR and dsXR were determined according to reported methods (*4*, *9*). If saturation in substrate was not achieved in the experiment (e.g., because of limited solubility of the aldehyde or weak apparent binding), the catalytic efficiency ($k_{cat}/K_{aldehyde}$) was obtained from the part of the Michaelis−Menten curve where the initial rate is linearly dependent on the substrate concentration. Initial rates were recorded spectrophotometrically under conditions in which the concentration of aldehyde was varied and NADPH or NADH was present at a constant and saturating concentration of 220 μM.

A full set of kinetic parameters for the reaction in eq 1 was obtained

$$\text{D-xylose} + \text{NAD(P)H} + \text{H}^+ \leftrightarrow \text{xylitol} + \text{NAD(P)}^+ \quad (1)$$

from initial-rate measurements in the forward direction (xylose reduction) and reverse direction (xylitol oxidation) at 25 °C and pH 7.0 and nonlinear fits of data to eq 2

$$V = k_{cat}[E][A][B]/\{K_{iA}K_B + K_B[A] + K_A[B] + [A][B]\} \quad (2)$$

where V is the initial rate; $[E]$ is the molar concentration of enzyme subunits (36 kDa) (*9*); $[A]$ and $[B]$ are molar coenzyme concentrations [NAD(P)H; $NAD(P)^+$] and substrate concentrations (D-xylose; xylitol), respectively; K_{iA} is the apparent dissociation constant of the enzyme-coenzyme complex (μM); and K_A and K_B are Michaelis constants (μM; mM) for *A* and *B*, respectively. Inhibitor binding studies in which $NAD(P)^+$ and NAD(P)H served as product inhibitors of, respectively, the enzymic reduction of xylose and oxidation of xylitol were carried out essentially as described by Neuhauser et al. (*10*). Initial rates were fitted to the Michaelis−Menten equation expanded as required to incorporate inhibition by a competitive, mixed-type, or uncompetitive inhibitor (*10*).

pH studies were carried out in the direction of NAD(P)H-dependent xylose reduction. Experiments were performed in 50 mM potassium phosphate buffer (pH range 5.0−7.0) and 50 mM Tris/HCl (pH range ≥7.0−9.5). Initial rates were acquired under conditions in which [xylose] was varied and [NADH] or [NADPH] was constant and saturating (>5 $K_{NAD(P)H}$). pH profiles of log k_{cat} and log(k_{cat}/K_{xylose}) that were level below pK_b and decreased above pK_b were fitted to eq 3. pH profiles were fitted to eq 4 when log k_{cat} or log(k_{cat}/K_{xylose}) decreased both below pK_a and above pK_b.

$$\log Y = \log[Y_{max}/(1 + K_b/[H^+])] \quad (3)$$

$$\log Y = \log[Y_{max}/(1 + [H^+]/K_a + K_b/[H^+])] \quad (4)$$

In eqs 3 and 4, Y is k_{cat} or k_{cat}/K_{xylose}, Y_{max} is the maximum value of Y, K_a and K_b are macroscopic dissociation constants, and $[H^+]$ is the proton concentration. Suitable control experiments showed that msXR and dsXR were stable in the chosen pH range over the time of the assay (<5 min). Initial-rate measurements in the overlapping pH range of Tris and phosphate buffer (pH 7−8) revealed clearly that the buffer is not a source of observable pH dependencies of the kinetic parameters.

RESULTS AND DISCUSSION

Kinetic Characterization of D-Xylose Reduction by msXR and dsXR. To provide a basic comparison of msXR and dsXR with regard to their function in D-xylose reduction (eq 1), we carried out a full steady-state kinetic analysis for each isozyme and measured initial rates for NAD(P)H-dependent reduction of D-xylose and $NAD(P)^+$-dependent oxidation of xylitol at 25 °C and pH 7.0. Two separate sets of kinetic experiments were conducted with dsXR using either NADP(H) or NAD(H) as coenzyme of the enzymic oxidoreduction. Initial rates were obtained under conditions in which the substrate D-xylose (20−200 mM) or xylitol (20−940 mM) was varied at five different levels using four to five constant concentrations of coenzyme NAD(P)H (10−205 μM) or $NAD(P)^+$ (38−600 μM). In both reaction directions of eq 1, Lineweaver−Burk plots of the reciprocal initial rates versus the reciprocal substrate concentrations yielded four to five straight lines, each corresponding to a single coenzyme concentration, that intersected to the left of the ordinate axis (not shown). This pattern of the lines is indicative of a reaction mechanism in which a ternary complex between enzyme, coenzyme, and substrate must be formed before the first product is released (*10*).

In consideration of precedent in the literature (*10*−*13*), our assumption was that the kinetic mechanisms of msXR and dsXR would likely be ordered such that NAD(P)H binds before D-xylose and that xylitol is released before $NAD(P)^+$. Determination of the complete steady-state kinetic mechanism of each isozyme was, clearly, beyond the goal of this work. However, a basic series of inhibitor binding studies were carried out with the aim of supporting the above working hypothesis. For msXR, $NADP^+$ behaves as a competitive inhibitor against NADPH (K_i = 25 ± 4 μM). Likewise, NADPH is a competitive inhibitor against $NADP^+$ (K_i = 20 ± 5 μM). Competitive inhibition of NADPH versus $NADP^+$ and vice versa was observed both at unsaturating (<$K_{substrate}$; see later) and saturating concentrations of xylose and xylitol, respectively. An identical inhibition pattern

Table 1. Kinetic Parameters for msXR and dsXR at 25 °C and pH 7.0

parameter	msXR	dsXR (NADH)	dsXR (NADPH)
k_{catR}[a] (s^{-1})	28 ± 1	16 ± 1	16.3 ± 0.5
K_{xylose} (mM)	77 ± 12	30 ± 8	64 ±8
$K_{NAD(P)H}$ (μM)	28 ± 4	30 ± 6	19 ± 2.5
$K_{iNAD(P)H}$ (μM)	20 ± 5	8.1 ± 0.9	14 ± 6.8
k_{catR}/K_{xylose} (M^{-1} s^{-1})	360 ± 44	530 ± 114	250 ± 26
k_{catO}[a] (s^{-1})	0.6 ± 0.02	0.9 ± 0.02	0.8 ± 0.01
$K_{xylitol}$ (mM)	480 ± 40	40 ± 5	160 ±10
$K_{NAD(P)^+}$ (μM)	16 ± 3	37 ± 5	31 ± 3
$K_{iNAD(P)^+}$ (μM)	25 ± 4	74 ± 22	53 ± 9
$k_{catO}/K_{xylitol}$ (M^{-1} s^{-1})	1.3 ± 0.06	23 ± 2	5 ± 0.3
K_{eq}[b]	360	220	190

[a] R, aldehyde reduction; O, alcohol oxidation. [b] Calculated from the experimental parameters using the Haldane relationship $K_{eq} = (k_{catR}/K_{xylose})K_{iNAD(P)^+}/\{(k_{catO}/K_{xylitol})K_{iNAD(P)H})\}$; standard deviations for K_{eq} are ≤30% of the reported values.

was observed for dsXR using NADH ($K_i = 8 \pm 1$ μM) and NAD^+ ($K_i \approx 100$ μM) as the inhibitors of the reverse and forward reaction directions, respectively. These data imply the formation of binary complexes between msXR and NADPH or $NADP^+$ and between dsXR and NADH or NAD^+, as required by the ordered mechanism in which coenzyme binds first and substrate second. The apparent dissociation constants of the binary complexes are given by the K_i values.

Initial-rate data for D-xylose reduction and xylitol oxidation were fitted to eq 2 with the assumption of an ordered kinetic mechanism. Results are summarized in **Table 1**. The internal consistency of the kinetic parameters was checked by using the Haldane relationship, as shown in the footnotes of **Table 1**. The calculated values of between 190 and 370 for the equilibrium constant (K_{eq}) at pH 7.0 and 25 °C compare reasonably to an experimentally observed value of ≈400 (±20%) under these conditions. K_i values for NADP(H) and $NAD(P)^+$ thus obtained (**Table 1**) agree well with K_i values derived from inhibition experiments.

The data in **Table 1** provide a basic set of kinetic parameters of msXR and dsXR needed for a comparative analysis of isozyme function. On the basis of the expression $k_{catR}/(K_{iNAD(P)H}K_{xylose})$, we conclude that dsXR prefers NADH 3.6-fold over NADPH. Considering data in the literature indicating a 5−10-fold preference of dsXR for NADPH over NADH (reviewed in refs *1*, *6*, and *7*; *10*), this is an unusually high and thus unique specificity for NADH! Jeffries and co-workers reported XR activities in the yeast *Candida boidinii* that were higher with NADH than NADPH as cosubstrate (*14*). However, the *C. boidinii* XR system has not been explored biochemically. Because k_{catR}/K_{xylose} is much greater (>20-fold) than $k_{catO}/K_{xylitol}$ in all shown cases, we do not consider oxidation of xylitol to be a relevant reaction catalyzed by msXR or dsXR under any physiological boundary conditions. Comparison of K_{iNADPH} and K_{iNADP+} values for msXR indicates that NADPH and $NADP^+$ bind to this enzyme with nearly identical apparent affinities. Now, the ratio of the intracellular concentrations of NADPH and $NADP^+$ in sugar-metabolizing yeast will always be such that NADPH is present in excess (*15*). Therefore, msXR will generally be primed for reductive metabolism of xylose, and product inhibition by $NADP^+$ will not be significant. An analogous conclusion can be drawn for dsXR utilizing NADPH, considering the K_{iNADPH}/K_{iNADP+} ratio of 3.8. An interesting result for dsXR is the 9−12-fold tighter apparent binding of NADH than NAD^+ ($K_{iNAD(H)}$). The characteristic ratios of $NADH/NAD^+$ and NADPH/NADH in glucose-limited anaerobic culture of baker's yeast are approximately 0.15 and 2.8, respectively (*15*). Arguing by analogy to *S. cerevisiae* because data for *C. intermedia* are not available, the K_{iNADH}/K_{iNAD+} ratio seen for dsXR appears to be well matched to these in vivo conditions, which could prevail during xylose fermentation by *C. intermedia*. The observed K_{iNADPH}/K_{iNADH} ratio of 1.7 in dsXR is similar to the physiological ratio of the reduced nucleotides. On the basis of $k_{catR}/(K_{iNAD(P)H}K_{xylose})$ values and assuming that NADPH will act as competitive inhibitor with respect to NADH and vice versa, we can then estimate that dsXR-catalyzed xylose reduction under the fermentation conditions will take place using NADPH and NADH at similar rates.

Characterization of the Substrate Binding Sites of msXR and dsXR. Initial rates of aldehyde reduction by msXR and dsXR were measured using a series of sugars and related aldehyde substrates, as shown in **Tables 2** and **3**. If not stated otherwise, NADH was used as the coenzyme for dsXR-catalyzed reactions. However, we carried out control experiments in which NADPH was employed and reduction of unsubstituted straight-chain aldehydes by dsXR was measured. The relative substrate specificity of dsXR was not dependent on the coenzyme used. The substrate series was chosen such that the nonreacting parts of the aldehydes displayed a representative variation in respect to the number of carbon atoms, the extent to which the carbon chain was substituted with hydroxy groups, and the stereochemical orientation of the hydroxy groups present. It was expected that if the aldehyde-binding sites of msXR and dsXR differ significantly in their interactions with the selected substrates, an isozyme-related pattern of specificity will result and reveal the key components of individual substrate preference.

Apparent kinetic parameters for msXR and dsXR are summarized in **Tables 2** and **3**, respectively. Unless indicated otherwise, they were obtained from nonlinear fits of the initial-rate data to the Michaelis−Menten equation. As required for a realistic comparison of $k_{cat}/K_{aldehyde}$ values (*4*), the experimental catalytic efficiencies were corrected for the portion of free aldehyde present in an aqueous solution of the respective aldose (*16*) as it is the open-chain free-aldehyde form that is the true substrate of xylose reductase (*4*) (cf. **Tables 2** and **3**). Values of k_{cat}/K_{xylose} are identical for msXR and dsXR within the experimental error of ±15%. Hence, by the criterion of catalytic efficiency both enzymes are equally well qualified for xylose catabolism. $k_{cat}/K_{aldehyde}$ values for reduction of "good" substrates are in the range of 1000−3000 mM^{-1} s^{-1} and very similar for both isozymes. These include D-erythrose (four carbons); D-xylose and L-arabinose (five carbons); and L-idose and D-fucose (= 6-deoxy-D-galactose) (six carbons). msXR differs most significantly from dsXR (≈10-fold) in respect to catalytic efficiencies for reduction of unsubstituted straight-chain aldehydes, which are smaller for dsXR (**Tables 2** and **3**). Another interesting difference between the two isozymes is borne out by comparing enzymic reactions with D-glucose. dsXR displays a ≈10-fold specificity for the reduction of D-xylose over the reduction of D-glucose (**Table 3**). By contrast, D-glucose is about as good a substrate of msXR as is D-xylose (**Table 2**). Estimates for the intracellular levels of free D-xylose and D-glucose in *C. intermedia* are not available, but concentrations of free D-glucose in the cytosol are probably low due to the rapid conversion into D-glucose 6-phosphate, as was shown for the related yeast system *Saccharomyces cerevisiae* (*17*). It would seem unlikely, therefore, that D-glucose could compete with D-xylose to serve as a substrate of msXR.

For both isozymes, the value of $k_{cat}/K_{aldehyde}$ displays a strong dependence on the structure of the nonreacting substrate part, particularly the presence and configuration of hydroxy groups. In the case of msXR, the variation in catalytic efficiency across the series of pentoses and hexoses in **Table 2** is up to

Table 2. Apparent Kinetic Parameters of msXR for NADPH-Dependent Reduction of Polyhydroxylated and Other Aldehydes[a]

substrate	%[b]	$K_{aldehyde}$[c] (μM)	k_{cat} (s^{-1})	$k_{cat}/K_{aldehyde}$[c] ($mM^{-1}s^{-1}$)	$-\Delta\Delta G^{\#}$ of $k_{cat}/K_{aldehyde}$ (kJ/mol)
DL-glyceraldehyde	24.25	1140	24.3	21.3	13.5
propionaldehyde	100	78000	6.9	0.09	0.0
D-erythrose	4	33	24.3	736	16.5
butanal	100	23000	21.2	0.93	0.0
D-xylose	0.02	16	23.5	1470	13.9
D-lyxose	0.03			1.4[d]	–3.3
D-ribose	0.05	91	12.2	134	8.0
2-deoxy-D-ribose	0.01	38	1.4	36.8	4.8
L-arabinose	0.03	20	24.5	1230	13.5
L-lyxose	0.03	117	18.4	157	8.4
pentanal	100	3900	20.7	5.31	0.0
L-idose	0.1			3260[d]	14.5
D-glucose	0.0024	6	8.2	1370	12.3
2-deoxy-D-glucose	0.008	58	6.8	117	6.2
D-galactose	0.02	61	15.2	249	8.1
2-deoxy-D-galactose	0.03	221	8.4	38	3.4
D-fucose	0.007	10	20.7	2070	13.3
D-mannose	0.005			92[d]	5.6
hexanal	100			9.47[d]	0.0

[a] The NADPH concentration was 220 μM and saturating. Initial rates were determined in 50 mM potassium phosphate buffer, pH 7.0, at 25 °C. $\Delta\Delta G^{\#}$ was calculated according to eq 5. Standard deviations were <15%. [b] Content of free aldehyde in solution (*16*). [c] $K_{aldehyde}$ and $k_{cat}/K_{aldehyde}$ are corrected for the available portion of free aldehyde in solution. [d] Obtained from the linear part of the Michaelis–Menten curve.

Table 3. Apparent Kinetic Parameters of dsXR for NADH-Dependent Reduction of Polyhydroxylated and Other Aldehydes[a]

substrate	%[b]	$K_{aldehyde}$[c] (μM)	k_{cat} (s^{-1})	$k_{cat}/K_{aldehyde}$[c] ($mM^{-1}s^{-1}$)	$-\Delta\Delta G^{\#}$ of $k_{cat}/K_{aldehyde}$ (kJ/mol)
DL-glyceraldehyde	24.25	2425	14.1	5.8	12.7
propionaldehyde	100	132000	4.6	0.035	0.0
D-erythrose	4	20	27.5	1380	22.4
butanal	100	33000	5.4	0.16	0.0
D-xylose	0.02	10	16.9	1690	20.7
D-lyxose				3.3[d]	5.2
D-ribose	0.05	68	4.9	72	12.9
L-arabinose	0.03	28	13.5	482	17.7
L-lyxose	0.03	144	6.6	46	11.8
pentanal	100	14700	5.9	0.40	0.0
L-idose	0.1			1820[d]	19.5
D-glucose	0.0024	33	5.6	170	13.6
2-deoxy-D-glucose	0.008			36[d]	9.8
D-galactose	0.02	15	9.4	627	16.9
2-deoxy-D-galactose	0.03	126	3.5	28	9.2
D-fucose	0.007	7	10.2	1457	19.2
D-mannose	0.005			28[d]	9.0
hexanal	100			0.69[d]	0.00

[a] The NADH concentration was 220 μM and saturating. Initial rates were determined in 50 mM potassium phosphate buffer, pH 7.0, at 25 °C. $\Delta\Delta G^{\#}$ was calculated according to eq 5. Standard deviations were <15%. [b] Content of free aldehyde in solution (*16*). [c] $K_{aldehyde}$ and $k_{cat}/K_{aldehyde}$ are corrected for the portion of free aldehyde in solution. [d] Obtained from the linear part of the Michaelis–Menten curve.

1000-fold. Aside from variations in apparent $K_{aldehyde}$ value (37-fold), this reflects a significant variation in k_{cat} (up to 17-fold). The change of $k_{cat}/K_{aldehyde}$ across essentially the same series of substrates is ≈512-fold for dsXR. The observed variation in k_{cat} is also smaller for dsXR than it is for msXR (4.5-fold). A strong dependence of k_{cat} on aldehyde side-chain structure could occur if catalysis was a major rate-limiting step of the reaction of msXR. Poor substrates react slowly, and so both turnover number and catalytic efficiency will be small. In an alternative scenario, aldehydes are bound to msXR in two different ways, one that is productive and promotes the reaction and another that leads to a catalytically incompetent complex which must dissociate to regenerate the active enzyme bound to NADPH. If nonproductive binding takes place with certain substrates, the observed values of k_{cat} for reduction of these aldehydes will be smaller than they would be if the reactions occurred exclusively through productive pathways. In any case, the value of $k_{cat}/K_{aldehyde}$ represents an extrapolation to an infinitely small substrate concentration, that is, conditions in which nonproductive binding cannot occur. Therefore, it will always be an accurate indication of the catalytic efficiency. The k_{cat} values of msXR for reduction of straight-chain aldehydes are high (≈20 s^{-1}), whereas, at the same time, the corresponding specificity constants are among the lowest observed for this enzyme. Therefore, this suggests that nonproductive binding may occur during the reaction of msXR with certain aldehydes.

Comparison of the catalytic efficiency for reduction of a selected aldose with the catalytic efficiency for reduction of an unsubstituted straight-chain aldehyde displaying an equivalent number of carbon atoms (cf. **Tables 2** and **3**) is relevant. It can provide an estimate of the net contribution of the hydroxy groups in this aldose to the specificity of the enzymic reaction. We employ eq 5 to relate a ratio of two specificity constants to a differential Gibbs free energy that is derived from bonding with

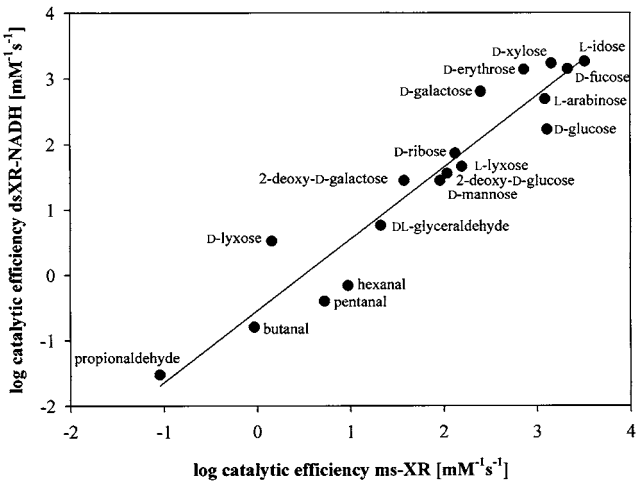

Figure 1. Quantitative structure–activity relationship analysis for the NADPH-dependent reduction of aldehydes by msXR and the NADH-dependent reduction of the same substrates by dsXR. The figure shows a log–log correlation of $k_{cat}/K_{aldehyde}$ values for msXR and dsXR. $k_{cat}/K_{aldehyde}$ values are taken from **Tables 2** and **3**. The solid line shows the fit of the data to a straight line.

the available hydroxy groups and used for transition-state stabilization

$$\Delta\Delta G^{\#} = -RT\ln(k_{cat}/K_{aldose}/k_{cat}/K_{straight-chain\ aldehyde}) \quad (5)$$

where R is the gas constant in J $K^{-1}mol^{-1}$ and T is the temperature in K. The calculated $\Delta\Delta G^{\#}$ values are found in **Tables 2** and **3**. Maximum transition state stabilization energies of 14 and 19−20 kJ/mol have been estimated for reactions catalyzed by msXR and dsXR, respectively. This result could imply that the catalytic efficiency of dsXR depends slightly more [≈6 kJ/mol (= 20 − 14)] on bonding interactions with sugar hydroxyls than that of msXR.

The data in **Tables 2** and **3** also show that 2-deoxy derivatives of sugars are generally much poorer substrates than the corresponding parent compounds (D-ribose, D-galactose, and D-glucose), all of which display a C-2(*R*) hydroxy group. A $\Delta\Delta G^{\#}$ value, which describes the differential binding energy stabilizing the transition state of the enzymic reaction with the parent sugar over the transition state for the same reaction with the corresponding 2-deoxy derivative, can be calculated using **Tables 2** and **3**. It is in a range of ≈4−6 kJ/mol. Therefore, this leads to the interpretation that non-covalent bonding with an appropriately oriented 2-OH contributes up to 43% of the maximum value of binding energy in the transition state of NAD(P)H-dependent aldehyde reduction by msXR and dsXR (i.e., 6 of 14 kJ/mol). Likewise, comparisons of enzymic reductions of sugars having *R*-configured C-2 with reductions of the corresponding C-2(*S*) epimers (D-xylose vs D-lyxose; D-glucose vs D-mannose) indicate that losses of transition-state stabilization energy in the C-2(*S*) substrates are almost identical to those in the 2-deoxy substrates. Therefore, aldose substrates diplaying an *R*-configured C-2 are preferred over their C-2 epimers, clearly because the substrate-binding sites provide favorable (likely hydrogen bonding) interactions with the C-2(*R*) hydroxy group, which are lacking in C-2(*S*) substrates. Non-covalent enzyme−substrate interactions at C-3 of the aldehyde are also important, as evident from comparisons of catalytic efficiencies for reductions of the C-3 epimers D-xylose and D-ribose or L-arabinose and L-lyxose.

Figure 1 shows a log−log correlation of $k_{cat}/K_{aldehyde}$ values for NADPH-dependent reduction of sugars by msXR with

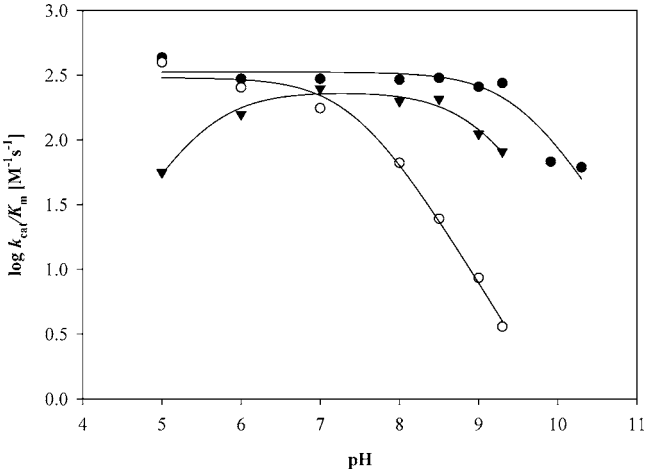

Figure 2. pH profiles of log k_{cat}/K_{xylose} for *C. intermedia* XR isozymes: **(●)** dsXR (NADH as coenzyme); (○) dsXR (NADPH as coenzyme); (▼) msXR (NADPH as coenzyme). $k_{cat}/K_{aldehyde}$ values were obtained from initial-rate data recorded in the presence of saturating coenzyme levels (200–250 μM) and are not corrected for the portion of free aldehyde in aqueous solutions of D-xylose. The solid lines are fits of the data to eq 3 or 4, as indicated in **Table 4**.

Table 4. p*K* Values from pH Profiles of log k_{cat}/K_{xylose} for msXR and dsXR

enzyme (coenzyme)	eq fitted	pK_a	pK_b	Y_{max} (M^{-1} s^{-1})
msXR (NADPH)	4	5.5 ± 0.1	9.0 ± 0.2	237 ± 21
dsXR (NADH)	3		9.5 ± 0.5	331 ± 39
dsXR (NADPH)	3		7.4 ± 0.1	302 ±36

corresponding specificity constants of dsXR using NADH as cosubstrate. This figure displays a simple comparative analysis of quantitative structure−activity relationships for dsXR and msXR. Its value is that it can measure similarities in the substrate-binding pockets of both enzymes or detect the absence of such similarities. **Figure 1** clearly suggests a relationship between the two sets of data that is linear overall. The data were fitted to a straight line, as shown in the figure, and a slope value of 1.10 and a correlation coefficient (r^2) of 0.912 were obtained from the linear fit. The interpretation of the structure−activity analysis is that binding modes for sugars are virtually identical at the substrate binding sites of msXR and dsXR.

pH Effects on Xylose Reduction by msXR and dsXR. Comparative pH studies for related enzymes catalyzing the same reaction can reveal subtle differences in pH-dependent ionization of groups involved in substrate binding and catalysis. Determination of pH effects on xylose reduction by msXR and dsXR was therefore considered to be potentially valuable. Apparent kinetic parameters for NADPH-dependent reduction of D-xylose by msXR and dsXR were obtained in the pH range of 5.0−9.5. k_{cat} and k_{cat}/K_{xylose} values for the NADH-dependent reaction of dsXR were determined in the pH range of 5.0−10.3. All pH profiles for log k_{cat} displayed a decrease at high pH that was either truly biphasic or had a marked hollow (*18*) in the pH range of 8.0−9.0 (not shown). pK_b values for the pH dependence of log k_{cat} were, therefore, not determined, and interpretation of these profiles would be speculative. Plots of log k_{cat}/K_{xylose} against pH are shown in **Figure 2** and reveal that, in all cases, activity decreases at high pH. Data were fitted to the appropriate equation, and results are summarized in **Table 4**. The pH profile for dsXR (using NADPH as coenzyme) decreases above an apparent pK_b value of 7.4. Interestingly, when NADH is employed as the coenzyme, a significantly higher apparent pK_b

value of 9.5 is observed. In the case of msXR, which obviously was assayed with NADPH, the pH profile decreases with a ±1 slope below an apparent pK_a of 5.5 and above another pK_b of 9.0. For the interpretation of the observed pH effects we must consider that NAD(P)H was saturating in the experiments and D-xylose does not show ionization in the used pH range. Therefore, the pH profiles of log k_{cat}/K_{xylose} reflect pH-dependent ionizations in binary enzyme−coenzyme complexes. Note that because [coenzyme] was saturating, the difference in pK_b value seen for NADH- and NADPH-linked reactions of dsXR cannot be attributed to a pH-dependent ionization of the 2′-phosphate group of free NADPH. The pH profiles reveal macroscopic pK_b values of groups required for D-xylose binding and/or catalysis. A picture of considerable similarity among XR isoforms emerges from the comparison of pH effects in **Figure 2** and **Table 4**; particularly, the pK_b values for msXR−NADPH and dsXR−NADH are the same within standard error. The lower pK_b seen in dsXR−NADPH, compared to dsXR−NADH, is not directly open to interpretation. However, the marked difference in pK_b could be explained if the ionizable groups showing in the two binary complexes were not the same or if the pK of the functional group(s) was in some way dependent on the 2′-phosphate group of NADPH. The intracellular pH of *C. intermedia* is not known. However, if we draw again analogy to baker's yeast and assume a probable in vivo pH value of 6.8 (*19*), msXR−NADPH and dsXR−NADH complexes are fully protonated and hence in the correct ionization state for xylose reduction. Under the assumed pH conditions, the dsXR−NADPH complex could be partly ineffective catalytically due to noticeable deprotonation. If that was truly the case, pH effects could contribute to a discrimination of dsXR against the use of NADPH.

Conclusions. Aside from the ability to utilize NADH in place of NADPH, the functional feature that distinguishes dsXR most from msXR is differential binding recognition of NADH versus NAD^+. The aldehyde-binding sites of the isozymes are very similar in regard to the non-covalent interactions that they can provide with a range of substrates and the pH-dependent ionization of functional groups on the protein. The physiological implication of binding NADH more tightly than NAD^+ is without doubt alleviating product inhibition by NAD^+, which will be present in excess over NADH at all times, even when during xylose fermentation respiratory chain-linked reoxidation of NADH is low. The fact that dsXR has a ≈4-fold higher specificity for NADH than NADPH could make this enzyme an interesting novel candidate to be used in metabolic engineering of the yeast xylose metabolism, likely in *S. cerevisiae* (*1*, *2*). We emphasize that this is the first XR enzyme found to prefer NADH. Obviously, increased levels of dsXR activity could contribute to an improvement of ethanol production from D-xylose by reducing the cofactor imbalance of the initial catabolic pathway.

ABBREVIATIONS USED

XR, xylose reductase; dsXR, dual NADH/NADPH-specific XR; msXR, NADPH-specific (monospecific) XR; XDH, xylitol dehydrogenase.

LITERATURE CITED

(1) Hahn-Hägerdal, B.; Wahlbom, C. F.; Gardonyi, M.; van Zyl, W. H.; Cordero Otero, R. R.; Jonsson, L. J. Metabolic engineering of *Saccharomyces cerevisiae* for xylose utilization. *Adv. Biochem. Eng. Biotechnol.* **2001**, *73*, 53−84.

(2) Jeffries, T. W.; Shi, N. Q. Genetic engineering for improved xylose fermentation by yeasts. *Adv. Biochem. Eng. Biotechnol.* **1999**, *65*, 117−161.

(3) Aristidou, A.; Penttilä, M. Metabolic engineering applications to renewable resource utilization. *Curr. Opin. Biotechnol.* **2000**, *11*, 187−98.

(4) Nidetzky, B.; Mayr, P.; Hadwiger, P.; Stütz, A. E. Binding energy and specificity in the catalytic mechanism of yeast aldose reductases. *Biochem. J.* **1999**, *344*, 101−107.

(5) Lunzer, R.; Mamnun, Y.; Haltrich, D.; Kulbe, K. D.; Nidetzky, B. Structural and functional properties of a yeast xylitol dehydrogenase, a Zn^{2+}-containing metalloenzyme similar to medium-chain sorbitol dehydrogenases. *Biochem. J.* **1998**, *336*, 91−99.

(6) Ellis, E. M. Microbial aldo-keto reductases. *FEMS Microbiol. Lett.* **2002**, *216*, 123−131.

(7) Lee, H. The structure and function of yeast xylose (aldose) reductases. *Yeast* **1998**, *14*, 977−984.

(8) Gardonyi, M.; Osterberg, M.; Rodrigues, C.; Spencer-Martins, I.; Hahn-Hägerdal, B. High capacity xylose transport in *Candida intermedia* PYCC 4715. *FEMS Yeast Res.* **2003**, *3*, 45−52.

(9) Mayr, P.; Brüggler, K.; Kulbe, K. D.; Nidetzky, B. D-Xylose metabolism by *Candida intermedia*: isolation and characterisation of two forms of aldose reductase with different coenzyme specificities. *J. Chromatogr. B: Biomed. Sci. Appl.* **2000**, *737*, 195−202.

(10) Neuhauser, W.; Haltrich, D.; Kulbe, K. D.; Nidetzky, B. NAD-(P)H-dependent aldose reductase from the xylose-assimilating yeast *Candida tenuis*. Isolation, characterization and biochemical properties of the enzyme. *Biochem. J.* **1997**, *326*, 683−692.

(11) Nidetzky, B.; Klimacek, M.; Mayr, P. Transient-state and steady-state kinetic studies of the mechanism of NADH-dependent aldehyde reduction catalyzed by xylose reductase from the yeast *Candida tenuis*. *Biochemistry* **2001**, *40*, 10371−10381.

(12) Rawat, U. B.; Rao, M. B. Purification, kinetic characterization and involvement of tryptophan residue at the NADPH binding site of xylose reductase from *Neurospora crassa*. *Biochim. Biophys. Acta* **1996**, *1293*, 222−230.

(13) Rizzi, M.; Erlemann, P.; Bui-Thanh, N.-A.; Dellweg, H.-W. Xylose fermentation by yeasts. 4. Purification and kinetic studies of xylose reductase from *Pichia stipitis*. *Appl. Microbiol. Biotechnol.* **1988**, *29*, 148−154.

(14) Vadenska, E.; Kuzmanova, S.; Jeffries, T. W. Xylitol formation and key enzyme activities in *Candida boidinii* under different oxygen transfer rates. *J. Ferment. Bioeng.* **1995**, *80*, 513−516.

(15) Anderlund, M.; Nissen, T. L.; Nielsen, J.; Villadsen, J.; Rydstrom, J.; Hahn-Hägerdal, B.; Kielland-Brandt, M. C. Expression of the *Escherichia coli pntA* and *pntB* genes, encoding nicotinamide nucleotide transhydrogenase, in *Saccharomyces cerevisiae* and its effect on product formation during anaerobic glucose fermentation. *Appl. Environ. Microbiol.* **1999**, *65*, 2333−2340.

(16) Angyal, S. J. The composition of reducing sugars in solution: Current aspects. *Adv. Carbohydr. Chem. Biochem.* **1991**, *49*, 19−35.

(17) Theobald, U.; Mailinger, W.; Baltes, M.; Rizzi, M.; Reuss, M. In vivo analysis of metabolic dynamics in *Saccharomyces cerevisiae*: I. Experimental observations. *Biotechnol. Bioeng.* **1997**, *55*, 305−316.

(18) Cleland, W. W. Determining the chemical mechanisms of enzyme-catalyzed reactions by kinetic studies. *Adv. Enzymol.* **1977**, *45*, 273−387.

(19) Shanks, J. V.; Bailey, J. E. Estimation of intracellular sugar concentrations in *Saccharomyces cerevisiae* using ^{31}P nuclear resonance spectroscopy. *Biotechnol. Bioeng.* **1988**, *32*, 1138−1152.

Received for review April 25, 2003. Revised manuscript received October 10, 2003. Accepted October 28, 2003. Financial support from the Austrian Science Funds (FWF Project P-15208-MOB) and from the European Commission (EU FAIR CT 96-1098) is gratefully acknowledged.

JF034426J